Int. J. Solids Structures, 1974, Vol. 10. pp. 1155–1170. Pergamon Press. Printed in Gt. Britain.

THE AXIALLY STRESSED LIM REACTION RAIL SUBJECTED TO A MOVING LOAD†

JOHN J. LABRA‡
ENSCO, Inc., 5408A Port Royal Road, Springfield, Virginia 22151, U.S.A.

(*Received* 18 *October* 1973; *revised* 1 *March* 1974)

Abstract—A recently developed high speed test track for the Linear Induction Motor (LIM) Vehicle at Pueblo, Colorado consists of a welded railroad track supplemented by a continuous reaction rail. Due to constrained thermal expansions, high axial compressive forces may occur in this rail. Since the reaction rail is a relatively slender plate, high axial forces may affect its lateral stability and dynamic characteristics. In this paper the stability of the reaction rail due to axial compressive force is studied first. Following this, the effect of axial forces upon the critical velocity of a moving lateral load is studied.

Included in the analysis are representations of the rail, both as an isotropic and orthotropic entity. The moving lateral load applied to the rail is assumed to be a concentrated force, acting first at the top of the reaction rail, and then at two arbitrary points.

INTRODUCTION

The response of railroad tracks to dynamic loads has been investigated by various authors. An early investigation by S. Timoshenko[1] considered the response of a rail under the action of a constant vertical force moving at constant velocity. He found that the critical velocity, v_{cr} was 1118 m.p.h. Since this critical velocity is far beyond even existing locomotive capabilities, he concluded the effect of dynamic loads on the deflection is negligible for existing railroad track.

However, with the more modern welded track, the possibility of high compressive forces in the track due to constrained thermal expansions exist, resulting in possible track instability.

Indeed, this is shown in a recent study by A. D. Kerr[2] concerning the effect of an axial force upon v_{cr} for an infinite beam resting on a Winkler foundation and subjected to a moving concentrated load. He found that as the axial force N approached the critical buckling load N_{cr}, the critical speed v_{cr} approached zero.

A related problem may be anticipated when considering the dynamic response of the LIM reaction rail used at the DOT test facility in Pueblo, Colorado. This rail which is part of the linear induction motor (LIM) is placed in a vertical mode between a standard track designed to carry the high speed LIM vehicle.

The reaction rail is a continuous entity, void of any expansion joints. Hence, the possibility of high compressive forces due to temperature variations is again very high. In order to prevent buckling, the reaction rail is mounted to the ties while at very high temperatures, so that except for extremely hot days, the rail will be axially in tension. However, a limit to

† Research supported by the U.S. Department of Transportation Grant DOT-FR-20064. Based on part of author's Ph.D. thesis submitted to New York University (Dec. 1972).

‡ Staff Scientist, ENSCO, Inc., Springfield, Virginia 22151, U.S.A.

what is called the "neutral" temperature must be prescribed to prevent rail failure on very cold winter days. It is therefore important to determine what increase beyond the neutral temperature is allowable before the LIM rail becomes unstable.

The weight of the LIM vehicle is supported by its wheels resting on the standard track (the LIM rail is connected to the ties supporting this track). It is assumed, in view of the relative light weight of the vehicle, that the compressive force induced in the LIM rail due to bending in the vehicle plane is negligible. Nevertheless, in addition to the thermally induced forces discussed above, the LIM rail is subjected to moving loads applied by the vehicle's linear induction motor with speeds up to 250 m.p.h. (It is subjected to axial forces induced by the propulsion of the vehicle and lateral loads due to the car's hunting motion.) It is therefore important to understand the dynamic response of the LIM rail due to these loads. The present paper studies the critical velocity of the LIM rail due to a moving load, as affected by the axial tensile or compressive forces in the LIM rail, as well as the resulting stresses in the rail.

The response of the rail due to propagating free waves is first investigated and is then compared with the response due to a moving lateral load. This load is represented both by a single concentrated force acting at the upper edge of the reaction rail, and also by two concentrated forces at some arbitrary height on the rail. The reaction rail is considered both as an isotropic and orthotropic entity.

The LIM rail at Pueblo, Colorado is rigidly fastened to cross-ties spaced 19 in. apart. In view of the closeness of these fasteners compared to the length of the track, the LIM rail is assumed to be an infinitely long cantilever plate, rigidly supported at the base and free of constraints at the rail head. C. W. MacGregor[3] treated the case of an infinite cantilever plate rigidly supported at one edge, free at the other, and loaded laterally by a concentrated static load at its free end. He assumed a Fourier integral solution for the lateral deflection, and determined this at various points along the plate by plotting for each point the integrand, and then computing approximately the area beneath the curve.

A more general study was made by T. J. Jaramillo[4]. He obtained an exact solution in terms of improper integrals for the lateral deflection due to a statically applied concentrated load acting at an arbitrary point. By means of contour integration he then transferred his solution into series form. His results agree closely with MacGregor's when he assumed the load to act at the free edge. F. Dymek[5] also used the same Fourier integral method as Jaramillo obtaining, in series form, a similar solution for the infinite cantilever plate subjected to a static concentrated load.

Recent studies on an infinite cantilever plate, representative of the LIM rail situation were conducted by E. C. Haight and W. A. Hutchens[6, 7]. In an attempt to determine the stresses in the LIM rail due to the motor's guidance forces, they analyzed the rail subjected to static loads, and showed the effect of axial pretensioning on both the stresses and deflections of the rail. Unable to obtain a closed form solution, they determined the lateral static deformation by a finite difference method. To find the accuracy of this method, they compared their solution with the exact solution by Jaramillo when the load is concentrated and acting at the free edge of the plate. They found their error in deflection to be less than 5 percent ([6] p. 20). (However, it should be noted that a close agreement in deflection does not imply a close agreement in stresses.)

Based on their extensive analysis (static principles) they concluded that pretensioning significantly reduces the maximum lateral deflection over the entire anticipated temperature range, increases the maximum stress level in the longitudinal direction, and decreases the

other stress components. They found that the LIM rail should be able to support, without plastic deformation, a lateral load up to 6140 lbs. This is based on: (1) the maximum stress criterion, which defines as the yield stress 27000 psi, and (2) their result that the maximum principle stress induced in the LIM rail is 4400 psi per 1000 lbs. of lateral load. It should be noted that the maximum stress criterion may not be applicable for the LIM rail. Secondly, it should be noted that the maximum stress value used is based on a static analysis. In the following it will be shown that, when dynamic loads are considered, dynamic stresses result which may be more than twice the statically predicted values.

PROPAGATION OF FREE WAVES THROUGH AN AXIALLY STRESSED LIM RAIL

Before analyzing the response of the reaction rail to dynamic loads, several results are required for the response of the rail due to a propagating free wave. The rail is represented as an infinite homogeneous and isotropic cantilever plate, rigidly fixed at its base and free from constraints at the top, as shown in Fig. 1. The equation of the plate is

$$D\nabla^4 w + N\frac{\partial^2 w}{\partial y^2} + \rho h\frac{\partial^2 w}{\partial t^2} = 0 \tag{1}$$

where D is the flexual rigidity of the plate, h is the thickness of the plate, N is the thermally induced axial load, ρ is the density of the plate, and w is the lateral deflection.

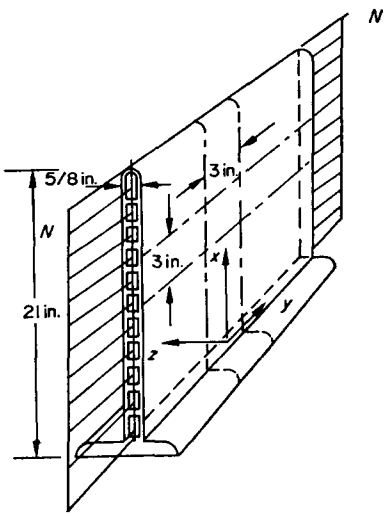

Fig. 1.

Using the wave type expression

$$w(x, y, t) = X(x)\cos\left[\frac{2\pi}{\lambda}(y - ct)\right] \tag{2}$$

in equation (1), X must satisfy the ordinary differential equation

$$\frac{d^4X}{dx^4} - 2\left(\frac{2\pi}{\lambda}\right)^2\frac{d^2X}{dx^2} + \left(\frac{2\pi}{\lambda}\right)^2\left[\left(\frac{2\pi}{\lambda}\right)^2 - \left(\frac{\rho hc^2 + N}{D}\right)\right]X = 0. \tag{3}$$

Assuming the case where

$$\frac{2\pi}{\lambda} = \alpha < \sqrt{\frac{N + \rho hc^2}{D}} \tag{4}$$

the solution to equation (3) is

$$X(x) = A_1 e^{\kappa_3 x} + A_2 e^{-\kappa_3 x} + A_3 \sin \kappa_4 x + A_4 \cos \kappa_4 x \tag{5}$$

where

$$\kappa_3 = \sqrt{\alpha\left[\alpha + \sqrt{\frac{N + \rho hc^2}{D}}\right]}; \quad \kappa_4 = \sqrt{\alpha\left[\sqrt{\frac{N + \rho hc^2}{D}} - \alpha\right]}. \tag{6}$$

The constants in (5) are determined from the boundary conditions of the plate. These are

$$\begin{aligned} w(0, y, t) &= 0; \qquad \left[\frac{\partial^2 w}{\partial x^2} + \nu \frac{\partial^2 w}{\partial y^2}\right]_{x=a} = 0 \\ \frac{\partial w}{\partial x}(0, y, t) &= 0; \qquad \frac{\partial}{\partial x}\left[\frac{\partial^2 w}{\partial x^2} + (2 - \nu)\frac{\partial^2 w}{\partial y^2}\right]_{x=a} = 0. \end{aligned} \tag{7}$$

These conditions represent the vanishing of the deflection and slope of the plate at its base and the corresponding moment and shear at the free edge ($x = a$).

We obtain, upon substitution of (2 and 5) into (7) four homogenous algebraic equations for the four unknowns (A_1, A_2, A_3, A_4). These four algebraic equations represent an eigenvalue problem with the phase velocity as the eigenvalue. Nontrivial solutions for the phase velocity exist only if the determinant of these equations is zero, i.e. when

$$\kappa_3 \kappa_4(\beta_3^2 + \beta_4^2)\cosh(\kappa_3 a)\cos(\kappa_4 a) + 2\kappa_3 \kappa_4 \beta_3 \beta_4 + (\kappa_4^2 \beta_3^2 - \kappa_3^2 \beta_4^2)\sinh(\kappa_3 a)\sin(\kappa_4 a) = 0 \tag{8}$$

where

$$\begin{aligned} \beta_3 &= \kappa_3^2 - \alpha^2 \nu; \qquad \gamma_3 = \kappa_3^3 - \alpha^2(2 - \nu)\kappa_3 \\ \beta_4 &= \kappa_4^2 + \alpha^2 \nu; \qquad \gamma_4 = \kappa_4^3 + \alpha^2(2 - \nu)\kappa_4 . \end{aligned} \tag{9}$$

In the following, equation (8) is evaluated for the LIM rail. The dimensions used for the LIM rail are shown in Fig. 1 and are as follows:

$$a = 21 \text{ in.}; \qquad h = 5/8 \text{ in.} \qquad (h \text{ is incorporated in } \kappa_3 \text{ and } \kappa_4)$$

Since the LIM rail is hollow, having longitudinal channels running along the length of the rail, it was decided to determine the rigidity experimentally. Two test sections were cut out of the LIM rail as shown in Fig. 1. Both sections were then simply supported on knife edges and loaded laterally by a concentrated force at mid span. Deflection curves were constructed and then compared with corresponding results of the classical beam theory. The elastic rigidities of the two sections were determined as

$$4{\cdot}8 \times 10^5 \text{ lb-in}^2 (EI_x); \qquad 5{\cdot}4 \times 10^5 \text{ lb-in}^2 (EI_y) \tag{10}$$

in the x and y directions respectively. Assuming a Poisson ratio of 0·3, the flexual rigidities of the plate in the x and y direction were determined as

$$D_1 = EI_x/t(1 - \nu^2) = 16{\cdot}8 \times 10^4 \text{ lb-in} \tag{11}$$

$$D_2 = EI_y/t(1 - \nu^2) = 18{\cdot}9 \times 10^4 \text{ lb-in} \tag{12}$$

where t is the width of the test sections. The difference between the two is quite small†. Because of this we may assume at first that the LIM rail is isotropic. Solutions for (α, c, N) satisfying (8) were computed for both rigidities, where α is a wave length parameter, c is the phase velocity and N is the thermally induced axial force.

Results satisfying (8) are plotted in Fig. 2 for various compressive and tensile axial forces. As found in [2], the minimum velocity of propagating free waves decreases as the compressive force increases. Conversely, when a tensile axial force is induced in the plate, the minimum velocity increases.

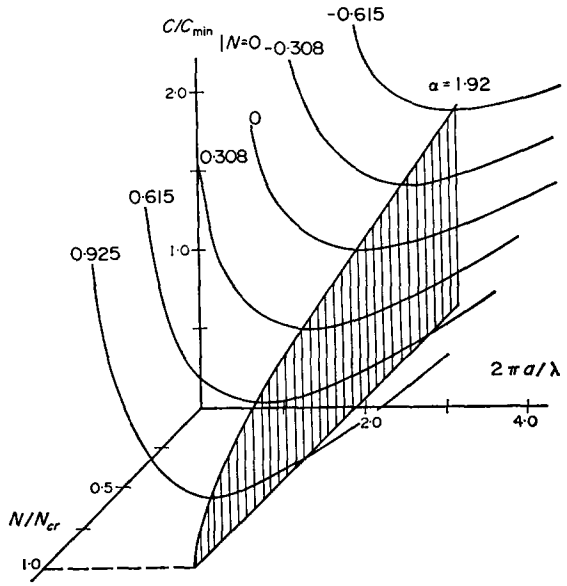

Fig. 2.

The minimum phase velocities of free waves corresponding to the two flexual rigidities when no axial force exists, were determined as

$$c_{\min} = 415 \text{ m.p.h. for } D_1; \qquad c_{\min} = 432 \text{ m.p.h. for } D_2. \tag{13}$$

One may also observe from studying Fig. 2 that independent of the axial forces and the flexural rigidity of the plate, the wave parameter corresponding to the minimum phase velocity of the propagating free waves is

$$\alpha a = \frac{2\pi a}{\lambda} = 1{\cdot}92. \tag{14}$$

Hence, for a LIM rail height of $a = 21$ in., the wave length $\lambda = 6$ ft. Also note from Fig. 2 that two wave trains with different wave lengths propagate with the same velocity, for $c > c_{\min}$.

† E. C. Haight and W. A. Hutchens[7] using the parallel-axis theorem determined for the LIM rail the flexual rigidity

$$D = 2E/(1-\nu^2)[t^3/12 + (e/2)^2] = 17{\cdot}9 \times 10^4 \text{ lb-in}$$

where t is the wall thickness and e is the distance between wall centerlines.

In the case when

$$\alpha > \sqrt{\frac{N + \rho hc^2}{D}} \tag{15}$$

it may be shown that the determinant of the corresponding four algebraic equations is non zero for all velocities. Hence, no wave trains of type (2) exist if (15) is satisfied.

CRITICAL VELOCITY FOR AXIALLY STRESSED LIM REACTION RAIL

In order to determine the v_{cr} for the LIM rail in the following, we consider the response of the rail subjected to a concentrated load P moving with a constant velocity and applied at the top of the rail (see Fig. 3). The governing equation describing the response of the rail is

$$D\nabla^4 w + N\frac{\partial^2 w}{\partial y^2} + \rho h\frac{\partial^2 w}{\partial t^2} = P\,\delta(y - ct)\,\delta(x - a). \tag{16}$$

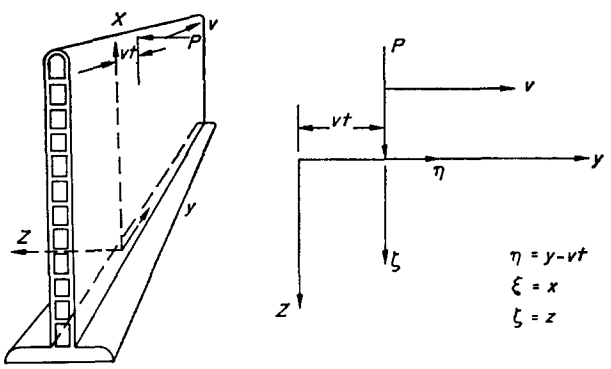

Fig. 3.

In problems of this nature it is assumed that a steady state exists for $v < v_{cr}$, as shown by J. Dörr[8]. His results confirmed the validity of the assumption that after a finite time, for $v < v_{cr}$, the transient vibrations vanish and the response of the beam to the moving load P approaches a steady state. This steady state assumption has also been applied to problems which include the effect of viscous damping, as seen in the study by J. T. Kenny[9]. He assumed the existence of a steady state response for a beam on an elastic foundation including damping, due to a load moving with a constant velocity. The damping assumption led to a finite displacement for $v = v_{cr}$.

In view of these studies, the existence of a steady-state response for (16) will be assumed. It is convenient to transform the stationary coordinates (x, y, z, t) to a moving set of coordinates (ξ, η, ζ) as shown in Fig. 3 where

$$\xi = x; \qquad \eta = y - vt; \qquad \zeta = z. \tag{17}$$

With this transformation, equation (16) reduces to

$$D\nabla^4 w + (\rho hv^2 + N)\frac{\partial^2 w}{\delta\eta^2} = P\,\delta(\eta)\,\delta(\xi - a). \tag{18}$$

It should be noted that due to the steady state assumption, P does not accelerate in the z direction, hence its inertial effect is zero. Therefore P in (18) only represents the static intensity of the load.

The corresponding boundary conditions are similar to (7), except for the non-homogeneity in the shear boundary condition at $\xi = a$. Considering this concentrated force P along the edge of the plate, we express its load distribution as the delta function of a Fourier cosine integral, since the load is symmetric. Hence, the shear distribution is taken as

$$V(y) = \frac{P}{\pi}\int_0^\infty \cos(\alpha y)\,\mathrm{d}\alpha. \tag{19}$$

The boundary conditions then reduce to

$$\begin{aligned} &w(0,\eta) = 0; \quad \frac{\partial^2 w}{\partial \xi^2}(a,\eta) + \nu\frac{\partial^2 w}{\partial \eta^2}(a,\eta) = 0 \\ &\frac{\partial w}{\partial \xi}(0,\eta) = 0; \quad \frac{\partial^3 w}{\partial \xi^3}(a,\eta) + (2-\nu)\frac{\partial^3 w}{\partial \xi\,\partial \eta^2} = \frac{-P}{\pi D}\int_0^\infty \cos(\alpha\eta)\,\mathrm{d}\alpha. \end{aligned} \tag{20}$$

Previous results for continuously supported beams without damping and subjected to moving loads, show that the response is even with respect to the load. Hence, w is assumed as a Fourier cosine integral.

$$w(\xi,\eta) = \int_0^\infty \chi(\alpha,\xi)\cos(\alpha\eta)\,\mathrm{d}\alpha. \tag{21}$$

Substituting this into (18) the D.E. is satisfied if

$$\frac{\mathrm{d}^4\chi}{\mathrm{d}\xi^4} - 2\alpha^2\frac{\mathrm{d}^2\chi}{\mathrm{d}\xi^2} + \alpha^2\left[\alpha^2 - \left(\frac{\rho h v^2 + N}{D}\right)\right]\chi = 0. \tag{22}$$

Equation (22) is identical to (3) where α now represents a parameter of integration, and v the velocity of the moving load P. Its solution is of the form

$$\chi(\xi) = A_1 e^{\kappa_3\xi} + A_2 e^{-\kappa_3\xi} + A_3 e^{\kappa_4'\xi} + A_4 e^{-\kappa_4'\xi} \tag{23}$$

where

$$\kappa_3 = \sqrt{\alpha\left[\alpha + \sqrt{\frac{N+\rho h v^2}{D}}\right]}; \quad \kappa_4' = \sqrt{\alpha\left[\alpha - \sqrt{\frac{N+\rho h v^2}{D}}\right]}. \tag{24}$$

Noting that κ_4' may be real or imaginary, depending whether

$$\alpha \lessgtr \sqrt{\frac{N+\rho h v^2}{D}} \tag{25}$$

we substitute (23 and 21) into (20) and obtain four algebraic equations in the four unknowns (A_1, A_2, A_3, A_4). Since the algebraic expressions are non homogeneous, a bounded solution exists if the determinant

$$\begin{vmatrix} 1 & 1 & 1 & 1 \\ \kappa_3 & -\kappa_3 & \kappa_4' & -\kappa_4' \\ \beta_3 e^{\kappa_3 a} & \beta_3 e^{-\kappa_3 a} & \beta_4' e^{\kappa_4' a} & \beta_4' e^{-\kappa_4' a} \\ \gamma_3 e^{\kappa_3 a} & -\gamma_3 e^{-\kappa_3 a} & \gamma_4' e^{\kappa_4' a} & -\gamma_4' e^{-\kappa_4' a} \end{vmatrix} \tag{26}$$

is non-zero, where

$$\beta_4' = \kappa_4'^2 - \nu\alpha^2; \qquad \gamma_4' = \kappa_4'[\kappa_4'^2 - \alpha^2(2-\nu)]. \tag{27}$$

Infinite deflections may occur if (26) is identically zero. As shown previously, this occurs when (4) is satisfied. Condition (4) is equivalent, noting (6 and 24), to

$$\kappa_4' = i\kappa_4. \tag{28}$$

With (28) the determinant (26) is identical to the left hand side of (8). Hence infinite deflections may occur when

$$\kappa_3\kappa_4(\beta_3^2 + \beta_4^2)\cosh(\kappa_3 a)\cos(\kappa_4 a) + 2\kappa_3\kappa_4\beta_3\beta_4 + (\kappa_4^2\beta_3^2 - \kappa_3^2\beta_4^2)\sinh(\kappa_3 a)\sin(\kappa_4 a) = 0. \tag{29}$$

Velocities for which $w \to \infty$ are denoted in the literature as "critical". What was the necessary condition for the existence of propagating free waves is now a condition for the infinite lateral deflection, by the linear theory, of an axially stressed plate due to a laterally moving load. Solutions satisfying (29) for both LIM rail rigidities (11 and 12) are in the same form as shown in Fig. 2. The corresponding critical velocities for $N = 0$ are the same as (13), i.e.

$$v_{cr|N=0} = 415 \text{ m.p.h. for } D_1; \qquad v_{cr|N=0} = 432 \text{ m.p.h. for } D_2. \tag{30}$$

The critical velocities for $N \neq 0$ are evaluated numerically by computer. As shown in Fig. 4, as the compressive force in the LIM rail increases, v_{cr} decreases. Conversely, a tensile axial force increases v_{cr}.

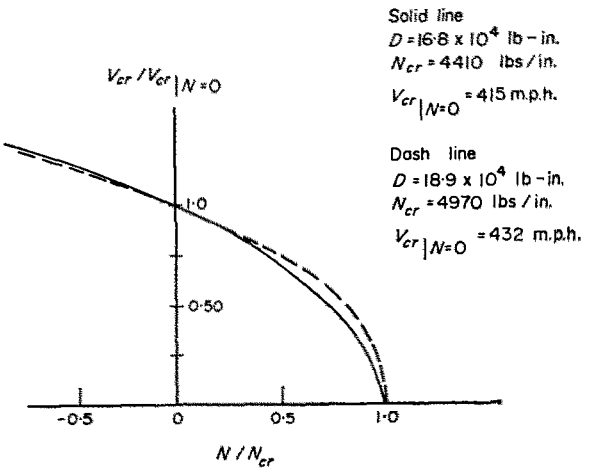

Fig. 4.

The deflection of the LIM rail as $v \to v_{cr}$, is determined by solving the constants (A_1, A_2, A_3, A_4) by means of Cramer's Rule, and substituting into expression (21). An example of the deflection pattern as $v \to v_{cr}$, which was solved on a computer, is shown in Fig. 5†.

† The computer program used may be found in the author's Ph.D. dissertation at New York University, 1972.

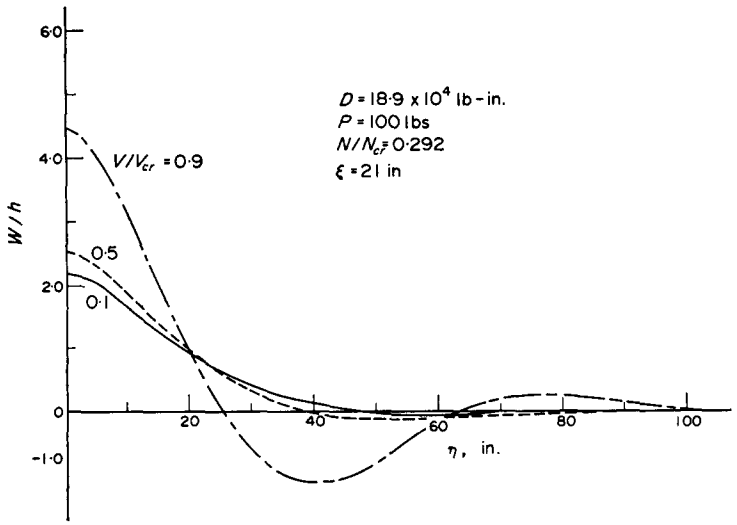

Fig. 5.

It is noted that due to the steady state and even response assumptions in the formulation, the analysis is being limited to $v < v_{cr}$. Earlier investigations by various authors on the subject of the response of continuously supported beams subjected to moving loads, verified the existence of a steady state for $v < v_{cr}$, and also the difference in solutions for the lateral response of the beam when $v < v_{cr}$ and $v > v_{cr}$.

STRESS ANALYSIS OF THE LIM RAIL

As stated in the introduction, one expects to find dynamic stresses in the LIM rail larger than those statically determined. The normal stresses, $\sigma_{\eta\eta}$ in the longitudinal direction and $\sigma_{\xi\xi}$ in the transverse direction, may be written

$$\sigma_{\eta\eta} = \frac{E(h/2)}{D(1-\nu^2)} M_\eta + \frac{N}{h}; \qquad \sigma_{\xi\xi} = \frac{E(h/2)}{D(1-\nu^2)} M_\xi \tag{31}$$

where the moment of inertia has been replaced by equivalent material constants since they were readily available from the experimental tests. M_ξ and M_η are the corresponding bending moments. In terms of the lateral displacement these bending moments are

$$M_\xi = -D\left[\frac{\partial^2 w}{\partial \xi^2} + \nu \frac{\partial^2 w}{\partial \eta^2}\right]; \qquad M_\eta = -D\left[\frac{\partial^2 w}{\partial \eta^2} + \nu \frac{\partial^2 w}{\partial \xi^2}\right]. \tag{32}$$

Substituting (21) into (32), the integral expressions where evaluated by computer using Simpson's rule along with the corresponding stresses (31).

The normal stresses were evaluated at a location directly under the load P, i.e. $\xi = 5$ in. and $\eta = 0$. The largest stresses at this point are shown in Fig. 6. It is shown that compared to static values the stresses approximately double as $v \to 0{\cdot}9 v_{cr}$.

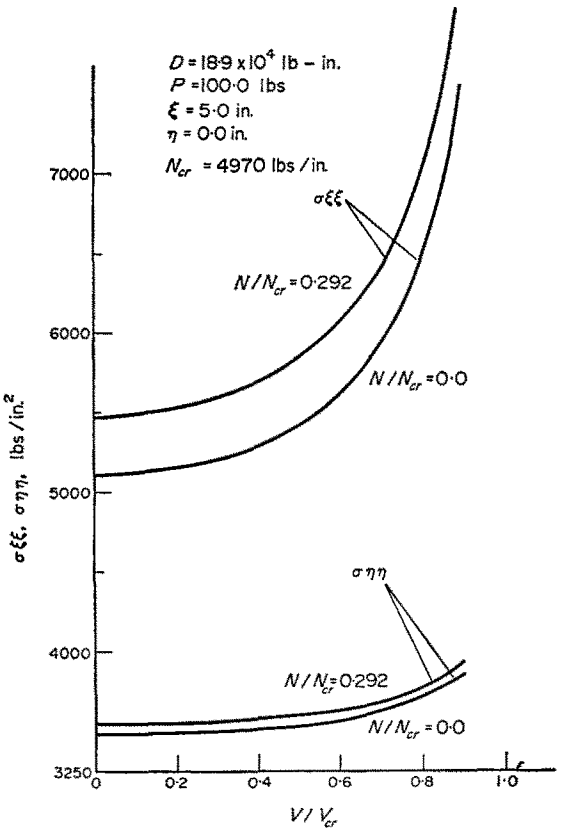

Fig. 6.

ANALYSIS OF THE LIM REACTION RAIL AS AN ORTHOTROPIC PLATE

In the previous study of the response of the LIM rail to dynamic loads, it was assumed that the rail was isotropic. Since the rail is actually hollow with internal web structure, (11 and 12) were determined experimentally as the two mutually perpendicular rigidities.

Due to these test results it is now assumed that the rail has three planes of symmetry with respect to its elastic properties. Due to this orthotropy, the corresponding differential equation is [10]

$$D_1 \frac{\partial^4 w}{\partial x^4} + 2D_3 \frac{\partial^4 w}{\partial x^2 \partial y^2} + D_2 \frac{\partial^4 w}{\partial y^4} + N \frac{\partial^2 w}{\partial y^2} + \rho h \frac{\partial^2 w}{\partial t^2} = 0 \tag{33}$$

where

$$D_1 = (EI)_x/t(1 - \nu^2); \qquad D_2 = (EI)_y/t(1 - \nu^2) \tag{34}$$

and D_3 corresponds to the torsional rigidity of the rail. If the parameters γ_1, γ_3 are introduced such that

$$D_2 = D; \qquad D_1 = \gamma_1 D; \qquad D_3 = \gamma_3 D \tag{35}$$

equation (33) may be written as

$$\gamma_1 \frac{\partial^4 w}{\partial x^4} + 2\gamma_3 \frac{\partial^4 w}{\partial x^2 \partial y^2} + \frac{\partial^4 w}{\partial y^4} + \frac{N}{D}\frac{\partial^2 w}{\partial y^2} + \frac{\rho h}{D}\frac{\partial^2 w}{\partial t^2} = 0. \tag{36}$$

The procedure is the same as for the isotropic plate. Substituting the wave expression

$$w(x, y, t) = X(x)\cos\left[\frac{2\pi}{\lambda}(y - ct)\right] \tag{37}$$

into (36) the D.E. is satisfied if

$$\gamma_1 \frac{d^4 X}{dx^4} - 2\gamma_3 \alpha^2 \frac{d^2 X}{dx^2} + \alpha^2\left[\alpha^2 - \left(\frac{N + \rho h c^2}{D}\right)\right]X = 0 \tag{38}$$

where $\alpha = 2\pi/\lambda$.

If the constraint

$$\alpha < \sqrt{\frac{N + \rho h c^2}{D}} \tag{39}$$

is assumed, the solution to (38) may be written as

$$X(x) = A_1 e^{\kappa_3 x} + A_2 e^{-\kappa_3 x} + A_3 \sin(\kappa_4 x) + A_4 \cos(\kappa_4 x) \tag{40}$$

where

$$\kappa_3 = \sqrt{\alpha\left[\alpha\frac{\gamma_3}{\gamma_1} + \sqrt{\frac{N + \rho h c^2}{\gamma_1 D} - \frac{\alpha^2(\gamma_1 - \gamma_3^2)}{\gamma_1^2}}\right]}$$

$$\kappa_4 = \sqrt{\alpha\left[\sqrt{\frac{N + \rho h c^2}{\gamma_1 D} - \frac{\alpha^2(\gamma_1 - \gamma_3^2)}{\gamma_1^2}} - \alpha\frac{\gamma_3}{\gamma_1}\right]}. \tag{41}$$

However, (40) has the same form of solution as was determined in the previously investigated isotropic case. Hence the existence of propagating free waves is assured if

$$\kappa_3 \kappa_4(\beta_3^2 + \beta_4^2)\cosh(\kappa_3 a)\cos(\kappa_4 a) + 2\beta_3 \beta_4 \kappa_3 \kappa_3 + (\beta_3^2 \kappa_4^2 - \beta_4^2 \kappa_3^2)\sinh(\kappa_3 a)\sin(\kappa_4 a) = 0. \tag{42}$$

This requires evaluation for the LIM rail. All parameters are the same as previously defined, with the exception of κ_3 and κ_4 which contain the additional parameters γ_1 and γ_3. γ_1 is the ratio of the rigidities for the LIM rail. According to the values in (11 and 12) it is 0·89.

If, the recommendation by S. G. Lekhnitskii (Ref. [11], p. 294) is accepted, the torsional rigidity may be equated to the smaller of the two experimentally evaluated rigidities, hence

$$\gamma_1 = \gamma_3 = 0{\cdot}89. \tag{43}$$

A more exact value may be found if the experimental method derived by R. K. Witt *et al.*[12] is used.

Substitution of (43) into (42) results in the dispersion equation for free waves through the axially stressed orthotropic LIM rail. When no axial force exists in the rail, the minimum velocity of propagation is found as

$$c_{\min} = 415 \text{ m.p.h.} \tag{44}$$

Except for the addition of the parameters γ_1, γ_3 the analysis for the orthotropic case is the same as the isotropic case. Hence, the details are not presented. The critical velocity will be found to equal the minimum phase velocity of propagating free waves through the LIM rail.

CRITICAL VELOCITY OF LIM RAIL FOR ARBITRARY POINT OF APPLIED LOAD

Previously, the response of a LIM rail subjected to a moving load located at the free edge of the plate was evaluated. Since the actual loads applied by the linear induction motor are located below the free edge, it would be of interest to generalize this problem by relocating the loads at some arbitrary point. It is of interest also to consider two concentrated loads instead of one, as shown in Fig. 7. This will come closer to simulating the actual loading by the motor, since the loads are transmitted by two sets of wheels a fixed distance apart.

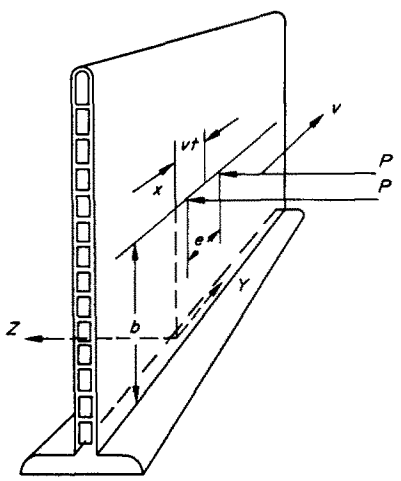

Fig. 7.

The governing differential equations are

$$\nabla^4 w_1 + \frac{N}{D}\frac{\partial^2 w_1}{\partial y^2} = 0; \qquad \begin{matrix} 0 \le x \le b \\ -\infty < y < \infty \end{matrix} \tag{45}$$

$$\nabla^4 w_2 + \frac{N}{D}\frac{\partial^2 w_2}{\partial y^2} = 0; \qquad \begin{matrix} b \le x \le a \\ -\infty < y < \infty \end{matrix} \tag{46}$$

where w_1 is the response of the LIM rail below the loads and w_2 is the response above. In terms of moving coordinates (ξ, η, ζ), (45 and 46) are written as

$$\nabla^4 w_1 + \left(\frac{N + \rho h v^2}{D}\right)\frac{\partial^2 w_1}{\partial \eta^2} = 0 \tag{47}$$

$$\nabla^4 w_2 + \left(\frac{N + \rho h v^2}{D}\right)\frac{\partial^2 w_2}{\partial \eta^2} = 0. \tag{48}$$

The corresponding boundary conditions are

$$w_1(0,\eta)=0; \qquad \left[\frac{\partial^2 w_2}{\partial\xi^2}+\nu\frac{\partial^2 w_2}{\partial\eta^2}\right]_{\xi=a}=0;$$

$$\frac{\partial w_1}{\partial\xi}(0,\eta)=0; \qquad \left[\frac{\partial^3 w_2}{\partial\xi^3}+(2-\nu)\frac{\partial^3 w_2}{\partial\xi\,\partial\eta^2}\right]_{\xi=a}=0;$$

$$w_1(b,\eta)=w_2(b,\eta); \qquad \frac{\partial w_1}{\partial\xi}(b,\eta)=\frac{\partial w_2}{\partial\xi}(b,\eta); \tag{49}$$

$$\left[\frac{\partial^2 w_1}{\partial\xi^2}+\nu\frac{\partial^2 w_1}{\partial\eta^2}\right]_{\xi=b}=\left[\frac{\partial^2 w_2}{\partial\xi^2}+\nu\frac{\partial^2 w_2}{\partial\eta^2}\right]_{\xi=b};$$

$$-\left[\frac{\partial^3 w_1}{\partial\xi^3}+(2-\nu)\frac{\partial^3 w_1}{\partial\xi\,\partial\eta^2}\right]_{\xi=b}+\left[\frac{\partial^3 w_2}{\partial\xi^3}+(2-\nu)\frac{\partial^3 w_2}{\partial\xi\,\partial\eta^2}\right]_{\xi=b}=V^*/D$$

where V^* is the nonhomogenuity in shear due to the applied lateral loads. This shear distribution may be represented, using Fourier integral theory, by the Fourier cosine integral

$$V^*(\eta)=\frac{2P}{\pi}\int_0^\infty \cos(e\alpha)\cos(\eta\alpha)\,\mathrm{d}\alpha \tag{50}$$

where e is the fixed distance between the loads.

As stated earlier, due to the results of previous studies on the response of continuously supported beams subjected to moving loads, the deflection of the rail is assumed as a Fourier cosine integral

$$w_1(\xi,\eta)=\int_0^\infty X_1(\alpha,\xi)\cos(\alpha\eta)\,\mathrm{d}\alpha \tag{51}$$

$$w_2(\xi,\eta)=\int_0^\infty X_2(\alpha,\xi)\cos(\alpha\eta)\,\mathrm{d}\alpha. \tag{52}$$

Substituting (51 and 52) into (47 and 48) we obtain

$$\frac{\mathrm{d}^4X_1}{\mathrm{d}\xi^4}-2\alpha^2\frac{\mathrm{d}^2X_1}{\mathrm{d}\xi^2}+\alpha^2\left[\alpha^2-\left(\frac{N+\rho hv^2}{D}\right)\right]X_1=0 \tag{53}$$

$$\frac{\mathrm{d}^4X_2}{\mathrm{d}\xi^4}-2\alpha^2\frac{\mathrm{d}^2X_2}{\mathrm{d}\xi^2}+\alpha^2\left[\alpha^2-\left(\frac{N+\rho hv^2}{D}\right)\right]X_2=0 \tag{54}$$

as the two ordinary differential equations which must be satisfied if (47 and 48) are to be satisfied. Solutions to (53 and 54) may be written in the form

$$X_1(\alpha,\xi)=A_1e^{\kappa_3\xi}+A_2e^{-\kappa_3\xi}+A_3e^{\kappa_4'\xi}+A_4e^{-\kappa_4'\xi} \tag{55}$$

$$X_2(\alpha,\xi)=B_1e^{\kappa_3\xi}+B_2e^{-\kappa_3\xi}+B_3e^{\kappa_4'\xi}+B_4e^{-\kappa_4'\xi} \tag{56}$$

where

$$\kappa_3 = \sqrt{\alpha\left(\alpha + \sqrt{\frac{N + \rho h v^2}{D}}\right)}; \qquad \kappa_4' = \sqrt{\alpha\left(\alpha - \sqrt{\frac{N + \rho h v^2}{D}}\right)}. \tag{57}$$

The solutions (55 and 56) are identical in form to (23). Substituting (55 and 56) into (51 and 52) results in

$$w_1 = \int_0^\infty [A_1 e^{\kappa_3 \xi} + A_2 e^{-\kappa_3 \xi} + A_3 e^{\kappa_4' \xi} + A_4 e^{-\kappa_4' \xi}]\cos(\alpha\eta)\, d\alpha \tag{58}$$

$$w_2 = \int_0^\infty [B_1 e^{\kappa_3 \xi} + B_2 e^{-\kappa_3 \xi} + B_3 e^{\kappa_4' \xi} + B_4 e^{-\kappa_4' \xi}]\cos(\alpha\eta)\, d\alpha \tag{59}$$

where $\kappa_4' = i\kappa_4$ when

$$\alpha < \sqrt{\frac{N + \rho h v^2}{D}}. \tag{60}$$

Substituting (58 and 59) into the boundary conditions results in eight algebraic equations for eight unknowns. Similar to the previous work on the LIM rail, it is found that critical velocities exist only when (60) is satisfied. In this case the determinant of the equations can be reduced to the product of two determinants

$$\Delta = \Delta_1 \Delta_2 \tag{61}$$

where Δ_1 and Δ_2, expanded are

$$\Delta_1 = -2(\beta_3 + \beta_4)(\gamma_3 \kappa_4 + \gamma_4 \kappa_3) \tag{62}$$

$$\Delta_2 = \kappa_3 \kappa_4(\beta_3^2 + \beta_4^2)\cosh(\kappa_3 a)\cos(\kappa_4 a) + 2\kappa_3 \kappa_4 \beta_3 \beta_4 + (\kappa_4^2 \beta_3^2 - \kappa_3^2 \beta_4^2)\sinh(\kappa_3 a)\sin(\kappa_4 a). \tag{63}$$

When (61) is identically zero, the deflection of the LIM rail may become infinite by the linear theory. Since it is of interest to find the critical velocity, one considers the case when

$$\Delta_1 \Delta_2 = 0. \tag{64}$$

Noting (9), Δ_1 may be written as

$$\Delta_1 = -2\kappa_3 \kappa_4(\kappa_3^2 + \kappa_4^2)^2 \tag{65}$$

which in non-zero for all values of (v, β, N). If (64) is to be satisfied, then

$$\Delta_2 = 0 \tag{66}$$

which is identical to (29). Hence the critical velocity when the load acts at an arbitrary point on the LIM rail is identical to the critical velocity when a concentrated load acts at the free edge of the rail.

CONCLUSION

The major result of this study is the significant effect that a lateral moving load may have upon the stability and stresses in the LIM reaction rail. It has been found that an induced axial force due to constrained thermal expansions may decrease the critical velocity of the reaction rail. This is shown in Fig. 4, where the static buckling loads are 7056 and 7952 psi

respectively. Here, a thermally induced compressive force whose magnitude is approximately 80 per cent of the static buckling load, will reduce the critical velocity of the LIM rail by 50 per cent. In terms of an equivalent temperature rise of the aluminum rail, the larger buckling load represents an increase of 61°F above the neutral temperature. This is based on a modulus of elasticity and thermal expansion coefficient of 10^7 psi and 13×10^{-6} in./in./°F respectively. Hence, while the critical velocity was found to be very high (430 m.p.h.) where no axial force exists in the rail, a nominal increase in temperature (50°F) will reduce the critical velocity by half (215 m.p.h.). This sensitivity which the critical speed has for temperature changes in the LIM rail emphasizes that care should be taken when choosing the setting or neutral temperature of the rail during construction of the track. Both minimum and maximum regional temperature extremes should be carefully considered.

Concerning the dynamic analysis of stresses in the LIM rail, it was found that the stresses more than doubled their static values when the velocity of the moving load approached v_{cr}. This is seen in Fig. 6 of the study. It can also be seen that the transverse stress ($\sigma_{\xi\xi}$) is more sensitive to the velocity changes than the longitudinal stress ($\sigma_{\eta\eta}$) as $v \to v_{cr}$. This is expected since the lateral deflection of the LIM rail increases as $v \to v_{cr}$.

As anticipated, the minimum velocity of propagating free wave through the LIM rail is equal to the rail's critical velocity. Its corresponding wave length was found to be 72 in. It is also noted from Fig. 5, that the nodal points of the deflection profile for the LIM reaction rail move toward the applied load as $v \to v_{cr}$, while the wave length of the bow wave decreases toward a lower limit of 72 in.

It was also determined in the study, that the critical velocity is independent of the number of applied concentrated loads or where they are located on the LIM rail. This is of interest since in the actual LIM motor configuration, there are four guide wheels which are located at fixed points beneath the upper edge of the reaction rail.

From the experimental tests for the rigidity of the LIM rail, it was found that anisotropy was minor for the purpose of determining the dynamic response of the reaction rail and hence, the assumption of isotropy may be applied. This simplifying assumption will aid any further studies on the LIM reaction rail which may be anticipated.

Acknowledgement—The author wishes to thank Dr. A. D. Kerr of New York University for his suggestion of the problem, and guidance in the writing of this paper.

REFERENCES

1. S. P. Timoshenko, Method of analysis of statistical and dynamical stresses in a rail, *Proc. 2nd Int. Cong. for Appl. Mech.*, Zurich, pp. 1–12 (1927).
2. A. D. Kerr, The continuously supported rail subjected to an axial force and moving load, *Int. J. Mech. Sci.* **14**, 71–78 (1972).
3. C. W. MacGregor, Deflection of a long helical gear tooth, *Mech. Engng* **57**, 225–227 (1935).
4. T. J. Jaramillo, Deflections and moments due to a concentrated load on a cantilever plate of infinite length, *J. appl. Mech.* 67–72 (March 1950).
5. F. Dymek, The infinite cantilever plate subjected to a concentrated load, *Rozprawy Inzynierskie* **3,11**, 411–42 (1963).
6. E. C. Haight and W. A. Hutchens, An approximate method for obtaining the lateral static deformation of a LIM reaction rail and observations on an equivalent lateral spring constant. The Mitre Corporation, *MTR*-4174, Vol. I (Oct. 15, 1970).
7. E. G. Haight and W. A. Hutchens, Stresses in the LIM reaction rail due to lateral and in-plane loads, The Mitre Corporation, *MTR*-4174, Vol. II (August 16, 1971).
8. J. Dörr, Dur unendliche, federnd gebettete balken unter dem Einfluss einer gleichmassig bewegten Last, *Ingenieur Archiv.* 167–192 (1943).
9. J. T. Kenny, Steady-state vibrations of beams on elastic foundations for moving loads, *J. appl. Mech.* 359–364 (1954).

10. S. P. Timoshenko, *Theory of Plates and Shells*, 2nd ed. pp. 364–368. McGraw-Hill.
11. S. G. Leknitskii, *Anisotropic Plates*, pp. 292–295. Gordon & Breach (1968).
12. R. K. Witt, W. H. Hoppmann and R. S. Buxbaum, Determination of elastic constants of orthotropic materials with special reference to laminates, *ASTM Bull.*, pp. 53–57 (Dec. 1953).

Абстракт — Недавно разработан испытательный путь большой скорости для Линейного Индукционного Моторного (ЛИМ) Поезда в Пуэбло, Колорадо состоит из сварной железнодорожной рельсовой пути и добавления в виде непрерывного рельса реагирования. Вследствие ограничения термических расширений, в этом рельсе могут возникать большие осевые сжимаемые усилья. Хотя рельс реагирования оказывается относительно гибкой пластинкой, большие осевые усилия могут затрагивать ее устойчивость плоской формы изгиба и динамические характеристики. В предлагаемой работе исследуется в первый раз устойчивость рельса реагирования вследствие сжимаемой силы. Следуя этому обсуждается эффект осевых усилий на критическую скорость движущейся поперечной нагрузки.

В анализе представляется рельс как изотропное так и ортотропные существо. Предполагается, что движущая поперечная нагрузка, приложенная к рельсу. Является сосредоточенной силой, которая действует с начала в верху рельса реагирования и далее, в двух произвольных точках.